

# The microstructures of silicon nitride/alumina ceramics

P. DREW, M. H. LEWIS

*Department of Physics, University of Warwick, Coventry, UK*

The microstructures of materials formed by sintering or hot-pressing mixtures of silicon nitride and alumina have been studied by transmission electron microscopy. The probable mechanism of transformation of the reactants to form  $\beta'$ -silicon aluminium oxynitride ( $\beta'$ -sialon) via a liquid phase sintering process, which is analogous to a similar transformation in hot-pressed silicon nitride containing a magnesia additive, is proposed. The origin and crystal symmetry of an unknown second phase is discussed. The residual quantity of this phase, known as the X-phase, is controlled mainly by the silica impurity content of the initial silicon nitride powder.

## 1. Introduction

It is now well known that the  $\beta$ - $\text{Si}_3\text{N}_4$  crystal structure can accommodate up to at least 60 wt %  $\text{Al}_2\text{O}_3$  by the substitution of Al on Si atomic sites and O on N sites, with only a small increase in the hexagonal unit cell parameters [1, 2]. In addition, other cations such as  $\text{Li}^+$  and  $\text{Mg}^{2+}$  can substitute in the structure [2, 3] leading to the possibility of a whole new range of ceramic materials. The development of these polycrystalline ceramics with good mechanical properties will depend not only on the intrinsic properties of the new crystalline phases but also on the grain size and the morphology and distribution of residual second phases which may result from the ceramic forming process.

This paper is concerned with a microstructural study of alumina-substituted materials ("sialons") which have been fabricated without the use of other additives by (a) the pressureless sintering of  $\text{Al}_2\text{O}_3/\text{Si}_3\text{N}_4$  compacts or (b) the hot-pressing of these mixtures.

## 2. Materials and experimental Techniques

Alumina and  $\alpha$ -silicon nitride powders (mean particle sizes  $< 2 \mu\text{m}$ ) were intimately mixed by alumina ball-milling in propanol for 24 h. A range of compositions and fabricating conditions were used to produce sialon materials from such mixtures. A hot-pressing apparatus, which has been described previously [4], was used to produce sialons containing between 10 and 60

wt % alumina with standard hot-pressing conditions of 1 ton in.<sup>2</sup> pressure at 1700°C for 1 h. A range of sintered materials were made in the graphite die of the hot-press without applying pressure. These contained 50 wt % alumina and were sintered for 1 h in the range 1400 to 1800°C. Large and rapid shrinkage accompanied the sintering to approaching theoretical density at the high temperatures, with severe cracking on cooling from 1800°C. This rapid shrinkage is evidence for a liquid-phase sintering process.

The experimental work consisted of an initial phase identification by the Debye-Scherrer X-ray method followed by a microstructural investigation by transmission electron microscopy. Thin slices of the bulk material, 0.2 mm thick, were cut on an annular diamond saw, glued to a brass block and ground to about 0.05 mm on silicon carbide papers. Thin foils for electron microscopy were produced by ion-beam sputtering, using 5 kV argon ions, incident on the specimen at 45°, for a period of 24 h.

## 3. Phase analysis by diffraction

### 3.1. X-ray diffraction

Debye-Scherrer X-ray photographs indicated the presence of two main crystalline reaction products in both types of material. The hot-pressed sialons were nearly single-phase substituted  $\beta$  with small amounts of an unknown crystalline phase present which is believed to be the same as that reported by Oyama [5] and by Jack and Wilson [1]. These two phases are

TABLE I

X-phase <i>d</i> -spacings (Å)	Comparison with Oyama [5]
7.86	—
5.58	—
3.63	3.62 and 3.66
3.01	3.02 and 3.04
2.80	2.80
2.61	2.62
2.27	2.28
1.43	1.43

henceforth referred to, after Jack, as the  $\beta'$ -phase and the X-phase respectively. The sintered material contained a relatively large quantity of the X-phase, indicated by the intensity of X-ray diffraction lines in the powder pattern. The *d*-spacings in Table I were measured from strong reflections of the X-phase using pure silicon as a diffraction standard.

In one specimen of a 20 wt % hot-pressed sialon the X-phase reflections were replaced by weak reflections which could be indexed on an orthorhombic lattice similar to the O' phases based on the structure of  $\text{Si}_2\text{N}_2\text{O}$  [6].

### 3.2. Electron diffraction

It was possible to obtain single crystal electron diffraction patterns from both  $\beta'$  and X grains using small selected-area apertures. Many patterns could be assigned to the  $\beta'$  hexagonal unit cell and the *d*-spacings from these patterns were used to determine the camera constant of the microscope. The remaining patterns were assigned to the X-phase structure and the data were used to compute the approximate parameters of the unit cell.

Fig. 1a, b and c shows three low index patterns consistently observed by selected-area diffraction from the X-phase. These patterns were tentatively indexed for [100], [010] and [001] zone axes respectively and the measured *d*-spacings corresponding to the various low index reflections are given in Table II.

The reciprocal lattice angles were measured from the diffraction patterns and are given by

$$\begin{aligned}\cos \alpha^* &= 109^\circ 5' \\ \cos \beta^* &= 96^\circ 14' \\ \cos \gamma^* &= 96^\circ 21'.\end{aligned}$$

These data indicate that the X-phase lattice is triclinic.

Comparing the results of the two diffraction methods, it is observed that many of the high

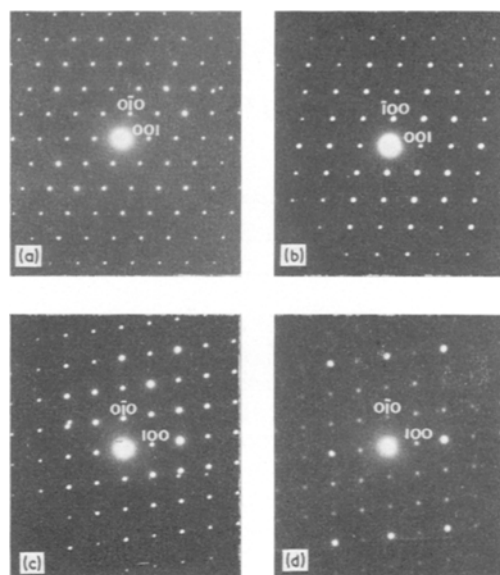


Figure 1 Selected-area diffraction patterns from the X-phase, containing low index reflections. (a), (b) and (c) are tentatively identified as having the [100], [010] and [001] zone axes respectively. In (d), which is the same pattern as (c), the superlattice effect is evident with comparatively strong reflections from the (200), (030) planes etc.

TABLE II

Figure	<i>d</i> -spacing (Å)	<i>hkl</i>
1a	9.11	010
	8.95	001
	7.80	011
	5.54	01 $\bar{1}$
1b	9.82	100
	8.95	001
	6.29	101
	7.02	10 $\bar{1}$
1c	9.82	100
	9.11	010
	6.35	110
	7.06	$\bar{1}10$

*d*-spacing reflections measured by electron diffraction are not detected by X-ray diffraction. It is believed that this arises from the occurrence of a "superstructure" in a compound of approximate composition  $\text{AlN} \cdot \text{SiO}_2$  [6] in which a typical silicate structure is modified by a partial substitution of nitrogen atoms for oxygen atoms. The "superlattice" effect may result either from an ordered distribution of the nitrogen and oxygen sites or of the aluminium

and silicon atoms. Jack [6] has suggested that the structure is related to that of "andalusite" ( $\text{Al}_2\text{O}_3 \cdot \text{SiO}_2$  - orthorhombic  $a = 7.79 \text{ \AA}$ ,  $b = 7.90 \text{ \AA}$ ,  $c = 5.56 \text{ \AA}$ ) which consists of isolated  $\text{SiO}_4$  tetrahedra linked by Al atoms in higher co-ordination i.e. the Al and Si positions are ordered and may be compared with the related "mullite" structure in which the Al and Si sites are disordered [7]. The X-ray reflections from the larger unit cell, possibly of lower symmetry than the basic disordered structure, are not observed due to low structure factors but the intensities of electron diffraction spots can be similar to the main diffraction spots in a 50 wt %  $\text{Al}_2\text{O}_3$  sialon or of lower intensity, as in Fig. 1d in the same material, probably due to local compositional variations and degrees of order in the X-phase. An apparent anomaly in Fig. 1c and d is the strong (200) reflection, which is also part of the reciprocal lattice for the basic structure but is not visible in the X-ray powder patterns ( $d$ -spacing  $\sim 4.9 \text{ \AA}$ ). However, the presence of other strong reflections from the basic structure will enhance the intensity of the (200) reflection in the electron diffraction pattern by multiple diffraction. The triclinic cell parameters of the X-phase were calculated to be approximately  $a = 9.9 \text{ \AA}$ ,  $b = 9.7 \text{ \AA}$ ,  $c = 9.5 \text{ \AA}$ ,  $\alpha = 109^\circ$ ,  $\beta = 95^\circ$ ,  $\gamma = 95^\circ$ . However, some electron diffraction patterns from grains within the same sialon contained anomalous spots which could not be indexed for a unit cell having these parameters. Thus, there exists the possibility of different "superlattice" cell sizes where the  $a$ ,  $b$  and  $c$  parameters are given by integral values of the dimensions of a smaller basic unit cell.

#### 4. Microstructures of sintered and hot-pressed sialons

Fig. 2 is a low magnification electron micrograph of the microstructure of a 50 wt %  $\text{Al}_2\text{O}_3$  material which had been sintered at  $1800^\circ\text{C}$  for 1 h. The microstructure contains many faceted  $\beta'$  grains, of the order of  $1 \mu\text{m}$  in size, which can be identified by selected area diffraction. The  $\beta'$  grains are surrounded by a matrix of the X-phase, which usually contains a large number of planar defects. Small areas of glass, which developed microscopic voids when exposed to 200 keV electrons [8], were occasionally observed, but this was not a basic feature of the microstructure. No alumina or  $\alpha$ -silicon nitride were detected although it is possible that small unreacted amounts were present.

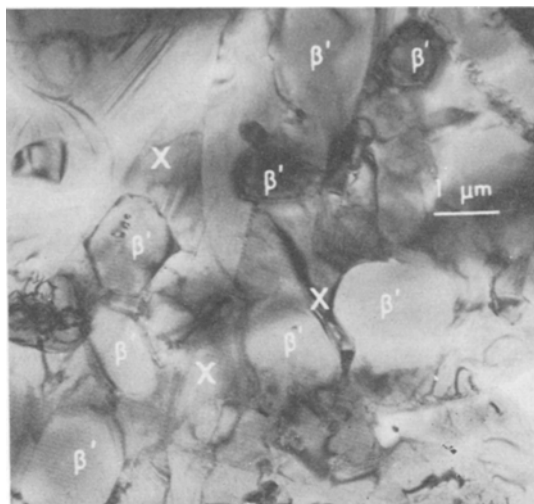


Figure 2 Low magnification micrograph of a sintered sialon, showing faceted  $\beta'$  grains situated in an X matrix.

The similar faceted shapes of most of the  $\beta'$  grains indicate that they have grown into a liquid phase at the sintering temperature. The grain morphology, which may be controlled partly by surface energy anisotropy and partly by growth kinetics, is determined with reference to Fig. 3. In Fig. 3a the projected shape of the right-hand  $\beta'$  grain approximates to that of a regular hexagon with the  $[0001]$  hexagonal  $\beta'$  direction normal to the projection plane (see inset diffraction pattern). The  $\beta'$  grain in Fig. 3b is perpendicular to the grain in (a) (indicated by the  $[10\bar{1}0]$  inset diffraction pattern) and illustrates the projected shape in this direction. Thus, the characteristic shape is that of a hexagonal prism of large elevation having rounded ends which may be composed of multiple small facets. Only those grains completely surrounded by the liquid phase at the sintering temperature show this precise morphology. Many  $\beta'$  grains have irregular shapes due to impingement upon other  $\beta'$  grains.

Materials sintered at  $1600$  and  $1700^\circ\text{C}$  had similar microstructures to the  $1800^\circ\text{C}$  sialon although the reaction was not as complete. The sialon sintered at  $1500^\circ\text{C}$  contains substantial amounts of unreacted alumina and  $\alpha$ -silicon nitride. Some regions of the microstructure of this material were very fine-grained, containing large numbers of  $\beta'$  grains less than  $0.1 \mu\text{m}$  in size. In all the sintered materials very few crystal defects were observed in the  $\beta'$  grains.

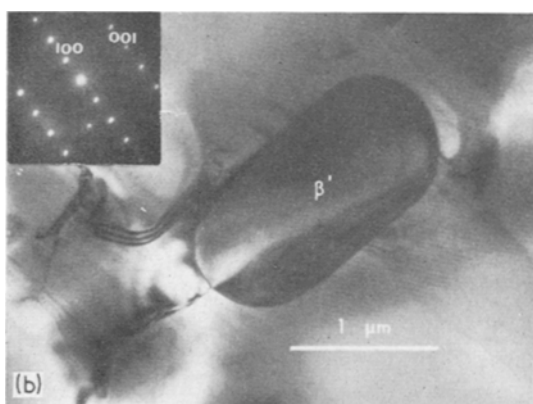
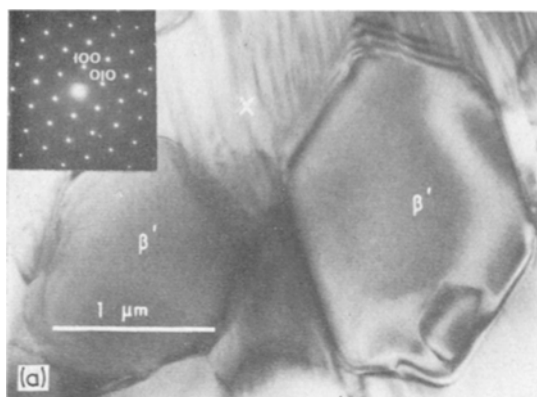


Figure 3 Sections through isolated  $\beta'$  grains in an X-phase matrix. (a) one of the grains is viewed in the [0001] direction and (b) in a  $[10\bar{1}0]$  direction.

The microstructures of the hot-pressed sialons were essentially single phase  $\beta'$  with a few isolated grains of X-phase. The micrograph of a 60 wt %  $\text{Al}_2\text{O}_3$  material in Fig. 4 illustrates the typical grain size of 0.2 to 1  $\mu\text{m}$ . Despite the lower proportion of X-phase, grains several microns across were quite common in the microstructure, as shown in Fig. 5a. The 20 wt %  $\text{Al}_2\text{O}_3$  material had a considerably smaller grain size, in the range 0.1 to 0.5  $\mu\text{m}$ .

The two types of planar imperfection observed in the X-phase are illustrated in Fig. 5a and b. Fig. 5a (from a hot-pressed material) shows thin lamellae of twinned crystal in weak diffraction contrast and in Fig. 5b anti-phase boundaries (APBs) are imaged in a large X-phase grain from the sintered material. These imperfections are normally present in varying density in all X-phase grains from either sintered or hot-pressed materials. Both twin and APB planes are parallel to (011) in the triclinic lattice but the

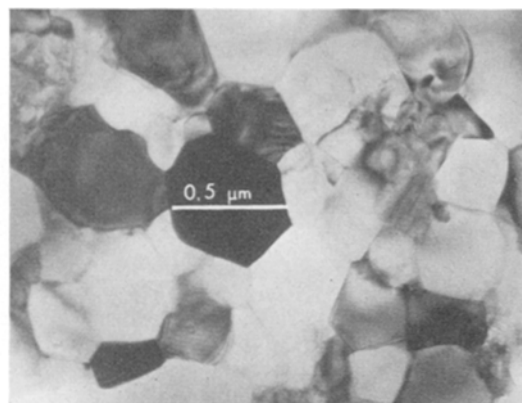


Figure 4 Microstructure of a hot-pressed sialon (60 wt %  $\text{Al}_2\text{O}_3$ ). Isolated grains of the X-phase are visible in a mainly  $\beta'$  grain structure.

APBs often deviate from this plane in curved form (Fig. 5b) and occasionally lie parallel to a secondary preferred plane near to (011).

An interpretation of these imperfections may be given with reference to the superlattice discussed in relation to the electron diffraction patterns. Thus, APBs are interfaces between X-phase crystal lamellae which are displaced relative to one another by a partial superlattice translation. The basic silicate type structure is continuous throughout these grains but aluminium or oxygen ordered sites are in anti-phase on either side of an APB. Twins represent two different superlattice orientations, i.e. two crystallographically equivalent distributions of the ordered species within the basic structure. The two alternative distributions result in slight distortions of the basic structure in opposite sense, giving rise to a weak contrast in bright-field images even when imaged with strong reflections due to the basic structure (Fig. 5a).

Both APBs and twins are believed to form as growth accidents either on solidification of the residual liquid of X-phase composition or via an order-disorder transformation during post-solidification cooling.

## 5. The densification and transformation process in sialons

The liquid phase produced during sintering (or hot-pressing) probably has a similar role to the liquid formed during the hot-pressing of silicon nitride with a magnesia additive [8]. After the initial stage of partial conversion to liquid during sintering (mainly via reaction of  $\text{Al}_2\text{O}_3$

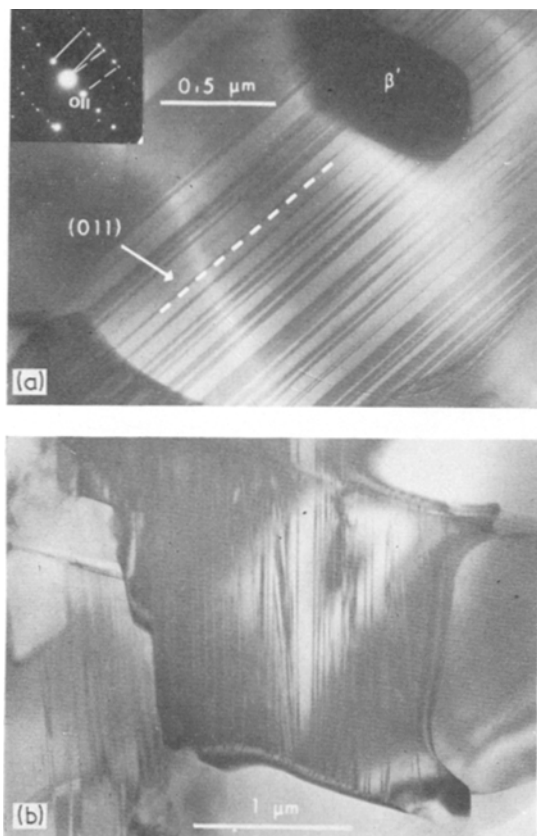


Figure 5 (a) Growth twins in the X-phase of a hot-pressed sialon (60 wt %  $\text{Al}_2\text{O}_3$ ). The broken and unbroken lines in the inset diffraction pattern indicate the separate patterns from twin related crystals. (b) Antiphase boundaries in the X-phase of a sintered material.

with surface  $\text{SiO}_2$ ) the nucleation of  $\beta'$  grains occurs at the many solid-liquid interfaces present. A dynamic process takes place in which the  $\alpha$ -silicon nitride and alumina reactants are progressively dissolved in the liquid and reprecipitated as  $\beta'$ -sialon. At the end of the process, the liquid of non-glass forming composition crystallizes on cooling to form the X-phase matrix. The higher volume fraction of X-phase in the sintered material, in comparison with the hot-pressed, indicates that the liquid contains a high silica content. The silica present in both types of material, which will control the amount of liquid production, results from the accidental oxidation of the  $\alpha$ -silicon nitride lath-like crystals which have a large total surface area. The proportion of silica in the sintered material may be increased by some oxidation in

\*  $10^3 \text{ psi} = 6.89 \text{ N mm}^{-2}$ .

the die during heating or by nitrogen dissociation at the sintering temperature when there is no applied pressure. Also, if the quantity of liquid phase diminishes as the reaction nears completion, this may contribute to the higher observed X-phase content of the sintered material. Even for comparable heat-treatment times, the reaction may be more rapid with application of pressure. It is evident from a comparison of microstructures in the hot-pressed and sintered materials, that the presence of a large liquid phase volume is detrimental to  $\beta'$  grain-size control. A possible explanation for this effect is the smaller nucleation rate for  $\beta'$  crystals in the presence of a large liquid volume. Thus the nucleation rate is controlled primarily by the concentration of silicon and nitrogen in the liquid phase. The nitrogen content of the liquid is derived from the  $\alpha$ -crystals, requiring larger numbers to dissolve in the initially alumino-silicate liquid before achieving the required supersaturation with respect to solid  $\beta'$  crystals. The effect is two-fold: in reducing the density of heterogeneous nucleation sites on  $\alpha$ -crystal surfaces and, probably more important, delaying the nucleation of new crystals during the growth of existing crystals, i.e. a decreased nucleation rate at lower "supersaturation". The presence of the X-phase can be eliminated [9] by the removal of silica. However, it is not known whether densification then involves (i) a liquid-phase sintering process in which a small quantity of liquid produces a residual glass or an undetectable amount of residual X-phase or (ii) a solid state-sintering process, which would require excessive temperatures to achieve a near theoretical density structure in reasonable times; at such temperatures the problems of dissociation or grain growth would be dominant.

The thermodynamics of the transformations occurring during the processing of silicon nitride ceramics are not completely understood. It is not certain that all samples of  $\alpha$ -silicon nitride contain as much oxygen as the samples examined by Grievson *et al.* [10]. Priest *et al.* [11] found, by neutron activation analysis, an oxygen content of  $0.3\% \pm 0.005\%$  in a pure sample of  $\alpha$  whereas the oxynitride structures require an oxygen content of 1% or more. The same authors heated  $\alpha$  to  $1800^\circ\text{C}$  at 275 psi\* inert gas pressure for 24 h without transformation to  $\beta$ . It is probable that  $\beta$  is the thermodynamically stable form at high temperatures

but there is a large activation energy for nucleation of  $\beta$  within solid  $\alpha$  due to the covalent nature of the bonding in silicon nitride. The solution of  $\alpha$  and reprecipitation as  $\beta$  (or  $\beta'$ ) silicon nitride through a silicate liquid provides a reaction path with a relatively low activation energy for nucleation.

Although  $\beta'$  and X were the major phases detected in the materials studied, there is evidence for the occurrence of other phases in the  $\text{Al}_2\text{O}_3\text{-Si}_3\text{N}_4\text{-SiO}_2$  ternary system. For example, a 50 wt %  $\text{Al}_2\text{O}_3$  sintered sialon was heat-treated in a graphite die by r.f. induction at  $1700^\circ\text{C}$  for 2 h in a helium atmosphere and quenched rapidly. X-ray and electron diffraction showed the presence of  $\beta'$ , an unidentified crystalline phase and a glass phase. Also, a compressed mixture of AlN and  $\text{SiO}_2$  in equal molar proportions was inductively heated in an iridium crucible for 30 min at  $1600^\circ\text{C}$  in a helium atmosphere; the resulting specimen contained a further unknown crystalline phase. Diffraction patterns from these new phases were distinguishable from that of the O' phase which was detected in a low  $\text{Al}_2\text{O}_3$  hot-pressed material. The formation and properties of new phases in the system  $\text{Si}_3\text{N}_4\text{-Al}_2\text{O}_3\text{-SiO}_2$  require further study. Of particular interest is the possibility of controlled crystallization of a Si-Al-O-N glass to form either  $\beta'$  or "nitrogen-silicate" type phases which have good intrinsic properties. Thus one would combine the advantages of good forming properties of a typical "glass-ceramic" with superior mechanical strength resulting from an enhanced degree of covalent bonding over pure silicate phases.\*

\*Lumby *et al.* [12] have recently shown that in the  $\text{AlN/SiO}_2/\text{Si}_3\text{N}_4$  ternary system single phase  $\beta'$  materials are only obtained on the composition line  $\text{Si}_{6-z}\text{Al}_z\text{N}_{8-z}\text{O}_z$ ; displacements from this line give rise to second phases.  $\text{Al}_2\text{O}_3/\text{Si}_3\text{N}_4$  materials fall off this composition line and are further displaced by silica impurity in the  $\alpha$ -silicon nitride. This explains the relatively large quantities of X-phase observed.

## Acknowledgements

We wish to thank Joseph Lucas Ltd for financial support of this work and for their permission to publish this paper. We are indebted to R. J. Lumby and R. R. Wills at the Group Research Centre, Monkspath, Solihull for the preparation of the sialon materials studied.

## References

1. K. H. JACK and W. I. WILSON, *Nature* **238** (1972) 80, 28.
2. Y. OYAMA and O. KAMIGAITO, *Jap. J. Appl. Phys.* **10** (1971) 1637.
3. *Idem*, *Yogyo Kyokai Shi* **81** (7) (1973) 290.
4. R. J. LUMBY and R. C. COE, *Proc. Brit. Ceram. Soc.* **15** (1970) 91.
5. Y. OYAMA, *Jap. J. Appl. Phys.* **12** (4) (1973) 500.
6. K. H. JACK, 17th Mellor Memorial Lecture, *Trans. and J. British Ceramic Soc.* **72** (1973) 376.
7. R. SADANAGA, M. TOKONAMI and Y. TAKEUCHI, *Acta Cryst.* **15** (1962) 65.
8. P. DREW and M. H. LEWIS, *J. Mater. Sci.* **9** (1974) 261.
9. K. H. JACK, private communication, March 1974.
10. P. GRIEVESON, K. H. JACK and S. WILD, "Special Ceramics 4" (edited by P. Popper) (British Ceramic Research Association, Stoke-on-Trent, 1972) pp. 385-93.
11. H. F. PRIEST, F. C. BURNS, G. L. PRIEST and E. C. SKAAR, *J. Amer. Ceram. Soc.* **56** (7) (1973) 395.
12. R. J. LUMBY, B. NORTH and A. J. TAYLOR, "Sialon Chemistry" presented at the special Ceramics Symposium, British Ceramic Research Association, Stoke-on-Trent, July 1974.

Received 15 May and accepted 10 July 1974.